Theoretical Mathematics & Applications, vol.5, no.1, 2015, 15-31
ISSN: 1792-9687 (print), 1792-9709 (online)
Scienpress Ltd, 2015

Approximate analytical Solution of Compressible Boundary Layer flow with an adverse Pressure Gradient by Homotopy Analysis Method

Nargund L. Achala[1] **and S.B. Sathyanarayana**[2]

Abstract

The aim of this work is to obtain approximate analytical solution to the two dimensional laminar compressible boundary layer flow with an adverse pressure gradient in the presence of heat and mass transfer. The method applied is homotopy analysis method. It is shown that this solution agrees very well with numerical solution which is obtained by Runge-Kutta Merson method and results are shown graphically for different magnetic parameters.Convergence of the solution is also discussed elaborately by using Domb Syke Plots.

Mathematics Subject Classification: 76N20
Keywords: Compressible boundary layer flow; Homotopy analysis method; Pade approximants; Alternate homotopy analysis method; Falkner Skan transformations

[1] Post Graduate Department of Mathematics and Research Centre in Applied Mathematics, MES College, 15th Cross, Malleswaram, Bangalore-560 003. E-mail: anargund1960@gmail.com
[2] Department of Mathematics, Vijaya College, R V Road, Basavanagudi, Bangalore-560 004. E-mail: sathya2864@yahoo.com

Article Info: *Received* : August 25, 2014. *Revised* : October 7, 2014.
Published online : January 10, 2015.

1 Introduction

Compressed air and gases are used in many industries such as automobile, chemical, food processing and mining industry for monitoring of pressurized spray lines and pumping of wheels in automobile industry. It is used for pneumatic conveying of granulate and powder, instrumentation, process air in the production, flushing processes and measurement of nitrogen in chemical industry and processing industries, and also for packaging and filling in food supply. It is used for pneumatic tooling in mining industries. Compressible fluid flow theory is used in the design of high speed aircraft, gas turbines, stream turbines, reciprocating engines, natural gas transmission lines and combustion chambers.

Chan et al.[6] developed an integral method for calculating the properties of compressible boundary layers with heat transfer and arbitrary pressure gradients. Venkatachala et al.[17] studied the flow and heat transfer for both cylinder and sphere moving in a compressible fluid at the stagnation point and was solved with quasilinearization technique on IBM 360 computer. Muthanna et al. [12] investigated the effect of surface mass and heat transfer velocities on the steady laminar, compressible boundary layer at a three dimensional stagnation point for both nodal and saddle points of attachment. Sau et al.[13] studied numerically the flow and heat transfer process on the unsteady flow of a compressible fluid which is viscous and with variable gas properties in the vicinity of the stagnation line of an infinite swept cylinder by quasilinearization technique with an implicit finite difference scheme. Ardeshir et al. [2] studied the transient growth in compressible boundary layers. Ali et al. [5] formulated and studied the problem of steady, laminar, compressible flow and heat transfer of a particulate suspension past a semi-infinite horizontal flat surface using finite-difference scheme. Hossain et al. [11] studied the effect of heat transfer on the steady laminar compressible boundary layer flow past a horizontal circular cylinder numerically by finite-difference scheme.

Kuerti [10] and Young [18] have given extensive review about compressible boundary layers. Curle [7] and Stewartson [16] have reported the details of special mathematical methods used by various authors. Some of the numerical approaches for solving compressible boundary value problems were discussed in the texts by Cebeci and Smith [4], Schreier [15] and Anderson [1]. In

Howarth's linearly retarded flow [8] strong adverse pressure gradient exists which will contribute to the increase in boundary layer and its thickness in the downstream flow. This will cause boundary-layer separation entails large energy losses. Therefore it is desired to prevent boundary-layer separation which can be done by suction [3], [4], [14]. Kafoussias et al. [9] studied the two dimensional laminar compressible boundary layer flow over a flat plate, with an adverse pressure gradient in the presence of heat and mass transfer numerically by Keller box method. We apply HAM and AHAM to Kafoussias model [9] and compare the results extensively by graphs.

2 Mathematical formulation of the problem

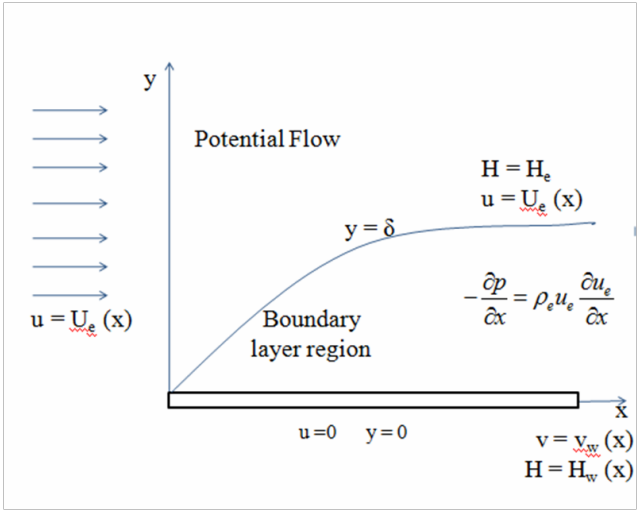

Figure 1: Flow Diagram

The equations governing the steady, compressible, two-dimensional boundary layer flow of a heat conducting perfect gas, which, in the absence of body forces, using Prandtl Boundary layer assumptions are [4], [9]

$$\frac{\partial}{\partial x}(\rho u) + \frac{\partial}{\partial y}(\rho v) = 0, \tag{1}$$

$$\rho u \frac{\partial u}{\partial x} + \rho v \frac{\partial u}{\partial y} = -\frac{dp}{dx} + \frac{\partial}{\partial y}\left(\mu \frac{\partial u}{\partial y}\right), \tag{2}$$

$$\rho u\frac{\partial H}{\partial x}+\rho v\frac{\partial H}{\partial y}=\frac{\partial}{\partial y}\left(\frac{\mu}{Pr}\frac{\partial H}{\partial y}+\mu\left(1-\frac{1}{Pr}\right)u\frac{\partial u}{\partial y}\right), \tag{3}$$

where H is the total enthalpy of the fluid defined for a perfect gas by the expression $H=C_pT+\frac{1}{2}u^2$, Pr is the Prandtl number defined as $\mathrm{Pr}=\frac{\mu C_p}{k}$ and the other quantities have their usual meaning.

Equations (1), (2) and (3) have five unknowns ρ, u, v, H and p. Thus we have three equations for five unknowns. p can be eliminated by using $u=u_e(x)$ and $\rho=\rho_e(x)$ in equation (2),

$$-\frac{dp}{dx}=\rho_e u_e\frac{du_e}{dx}, \tag{4}$$

where the subscript 'e' refers to the conditions at the edge of the boundary layer. Equation (2) can be written now as

$$\rho u\frac{\partial u}{\partial x}+\rho v\frac{\partial u}{\partial y}=\rho_e u_e\frac{du_e}{dx}+\frac{\partial}{\partial y}\left(\mu\frac{\partial u}{\partial y}\right). \tag{5}$$

The boundary conditions of the problem, including a transpiration velocity v_w at the wall are

$$y=0:\ u=0,\ v=v_w(x),\ H=H_w(x), \tag{6}$$

$$y\longrightarrow\delta:u=u_e(x),\ H=H_e, \tag{7}$$

where δ is the boundary layer thickness.

We introduce the compressible Falkner - Skan transformation and stream function defined by

$$\eta=\int_0^y\left(\frac{u_e(x)}{\nu_e(x)x}\right)^{1/2}\frac{\rho(x,y)}{\rho_e(x)}dy,\ \psi(x,y)=\left(\rho_e\mu_e u_e x\right)^{1/2}f(x,\eta), \tag{8}$$

Equations (1), (3) and (5) have four unknowns ρ, u, v and H. Equation (8) is used to eliminate one more unknown. ρ, u, v are absorbed in the stream function ψ, for a compressible flow given by

$$\rho u=\frac{\partial\psi}{\partial y},\ \rho v=-\frac{\partial\psi}{\partial x}, \tag{9}$$

which satisfy the continuity equation (1) exactly. Now we have two equations for two unknowns f and S. Equations (3), (5) and boundary conditions (6) and (7) reduce to

$$b\frac{\partial^3 f}{\partial\eta^3}+m_1 f\frac{\partial^2 f}{\partial\eta^2}+m_2\left(c-\left(\frac{\partial f}{\partial\eta}\right)^2\right)=x\left(\frac{\partial f}{\partial\eta}\frac{\partial^2 f}{\partial\eta\partial x}-\frac{\partial^2 f}{\partial\eta^2}\frac{\partial f}{\partial x}\right), \tag{10}$$

$$e\frac{\partial^2 S}{\partial \eta^2} + d\frac{\partial f}{\partial \eta}\frac{\partial^3 f}{\partial \eta^3} + d\left(\frac{\partial^2 f}{\partial \eta^2}\right)^2 + m_1 f\frac{\partial S}{\partial \eta} = x\left(\frac{\partial f}{\partial \eta}\frac{\partial S}{\partial x} - \frac{\partial S}{\partial \eta}\frac{\partial f}{\partial x}\right), \tag{11}$$

$$\eta = 0 : \frac{\partial f}{\partial \eta} = 0,\ f_w = f(0,x) = -\frac{1}{\left(u_e \mu_e \rho_e x\right)^{1/2}}\int_0^x \rho_w v_w(x)dx,\ S = S_w(x), \tag{12}$$

$$\eta = \eta_e : \frac{\partial f}{\partial \eta} = 1,\ S = 1, \tag{13}$$

where the quantities b, c, d, e, m_1 and m_2 are defined as follows

$$b = C,\ C = \frac{\rho\mu}{\rho_e\mu_e},\ c = \frac{\rho_e}{\rho},\ d = \frac{Cu_e^2}{H_e}\left(1 - \frac{1}{\mathrm{Pr}}\right),\ e = \frac{b}{\mathrm{Pr}},\ S = \frac{H}{H_e}, \tag{14}$$

$$m_1 = \frac{1}{2}\left[1 + m_2 + \frac{x}{\rho_e\mu_e}\frac{d}{dx}\left(\rho_e\mu_e\right)\right],\ m_2 = \frac{x}{u_e}\frac{du_e}{dx}. \tag{15}$$

So the problem under consideration is described by system of equations (10) and (11), with the boundary conditions (12) and (13), where as the coefficients in the equations are defined in (14) and (15). To apply homotopy analysis method, initially we do few assumptions for quantities in (14) and (15) which are treated as constants [14].

The influence of compressibility is contained directly in the density term ρ in the continuity equation (1), contained more indirectly as a variable coefficient in the momentum equation (2) and energy equation (3) and to produce temperature variations that are too large to permit the assumption of constant properties μ and k. The Prandtl number (Pr) is assumed nearly constant for most gases over a wide range of temperature. The pressure is assumed constant across the boundary layer. Therefore, the density can be assumed to be a function of temperature only.

We establish that

$$\frac{\partial f}{\partial \eta}\frac{\partial^2 f}{\partial \eta \partial x} - \frac{\partial^2 f}{\partial \eta^2}\frac{\partial f}{\partial x} = 0, \tag{16}$$

$$\frac{\partial f}{\partial \eta}\frac{\partial S}{\partial x} - \frac{\partial S}{\partial \eta}\frac{\partial f}{\partial x} = 0, \tag{17}$$

Using (16) and (17), the right hand sides of equations (10) and (11) vanish and $x \neq 0$. Thus these equations become

$$b\frac{\partial^3 f}{\partial \eta^3} + m_1 f\frac{\partial^2 f}{\partial \eta^2} + m_2\left(c - \left(\frac{\partial f}{\partial \eta}\right)^2\right) = 0, \tag{18}$$

$$e\frac{\partial^2 S}{\partial \eta^2} + d\frac{\partial f}{\partial \eta}\frac{\partial^3 f}{\partial \eta^3} + d\left(\frac{\partial^2 f}{\partial \eta^2}\right)^2 + m_1 f\frac{\partial S}{\partial \eta} = 0, \tag{19}$$

with boundary conditions

$$\eta = 0; f'(x,0) = 0, f_w = f(0,x) = -\frac{1}{(u_e\mu_e\rho_e x)^{\frac{1}{2}}}\int_0^x \rho_w v_w(x)dx, \;\; S = \omega \tag{20}$$

$$\eta = \eta_e; \;\; f'(x,\eta_e) = 1, \;\; S = 1. \tag{21}$$

3 Homotopy Analysis Method (HAM)

We solve equation (18) and (19) by homotopy analysis method by writing the given non linear equation as

$$N[f(\eta)] = b\frac{\partial^3 f}{\partial \eta^3} + m_1 f\frac{\partial^2 f}{\partial \eta^2} + m_2\left(c - \left(\frac{\partial f}{\partial \eta}\right)^2\right). \tag{22}$$

Homotopy for this equation is constructed as below

$$(1-p)L\left[f(\eta,p) - f_0(\eta)\right] = hp\left\{b\frac{\partial^3 f}{\partial \eta^3} + m_1 f\frac{\partial^2 f}{\partial \eta^2} + m_2\left(c - \left(\frac{\partial f}{\partial \eta}\right)^2\right)\right\}, \tag{23}$$

where

$$L = \frac{\partial^3}{\partial \eta^3} + \frac{\partial^2}{\partial \eta^2}, \tag{24}$$

with boundary conditions

$$F(0,p) = \lambda = f_w, \; \frac{\partial F}{\partial \eta}(0,p) = 0, \; \frac{\partial F}{\partial \eta}(\infty,p) = 1, \tag{25}$$

where $p\,\epsilon\,[0,1]$ is the embedding parameter, $h \neq 0$ is a non zero parameter. The initial guess approximation $f_0(\eta)$ of $f(\eta)$ chosen in accordance with boundary condition (12) and satisfying equation $Lf = 0$.

When p = 0, we have the solution

$$F(\eta,0) = f_0(\eta). \tag{26}$$

When p = 1,

$$F(\eta, 1) = f(\eta). \tag{27}$$

Thus as p increases from 0 to 1, the solution varies from the initial guess $f_0(\eta)$ to the exact solution $f(\eta)$. The initial guess approximation $f_0(\eta)$, the linear operator L and the parameter h are to be selected such that the equation (22) and (23) have solutions at each point $p\,\epsilon\,[0, 1]$ and the order of L must be same as that of N.

Using Maclaurin series for F(η,p) as

$$F(\eta, p) = F(\eta, 0) + \sum_{k=1}^{\infty} \frac{p^k}{k!} \frac{\partial^k}{\partial p^k}(F(\eta, p)), \tag{28}$$

and defining

$$\phi_0(\eta) = F(\eta, 0) = f_0(\eta), \tag{29}$$

we get

$$F(\eta, p) = \phi_0(\eta) + \sum_{k=1}^{\infty} \phi_k(\eta) p^k. \tag{30}$$

The convergence region of the above series depends upon the non-zero parameter h which is to be selected such that solution converges at p = 1. The values of h are chosen by drawing h graph by plotting $f''(0)$ versus h. Using equations (27), (29) and (30) for p = 1, we get

$$F(\eta, 1) = f(\eta) = \phi_0(\eta) + \sum_{m=1}^{\infty} \phi_m(\eta), \tag{31}$$

where $\phi_m(\eta)$ are the unknowns to be determined.

Differentiating equation (23) m times about the embedding parameter p, using Leibnitz theorem, setting p = 0 and dividing by m!, we get

$$L\left[\phi_m - \chi_m \phi_{m-1}\right] = h R_m(\eta), \tag{32}$$

where

$$\chi_m = \begin{cases} 0 \; when \; m \leq 1 \\ 1 \; when \; m > 1, \end{cases} \tag{33}$$

$$R_m[\eta] = b\phi'''_{m-1} + m_1 \sum_{k=0}^{m-1} \phi_{m-1-k} \phi''_k - m_2 \sum_{k=0}^{m-1} \phi'_{m-1-k} \phi'_k + m_2 c(1 - \chi_m), \tag{34}$$

with boundary conditions

$$\phi_m(0) = \phi_m^{'}(0) = \phi_m^{'}(\infty) = 0. \tag{35}$$

We solve these linear equations given by (32) for ϕ_m by MATHEMATICA and draw the graphs for different parameters.

Initial approximate solution, $f_0(\eta)$ is obtained as below by L and satisfying boundary conditions as

$$f_0(\eta) = \phi_0 = -1 + e^{-\eta} + \eta + \lambda, \tag{36}$$

and we get other ϕ's from (32) by using (36).

Equation (19) is also solved by homotopy analysis method by writing

$$N\left[S(\eta)\right] = e\frac{\partial^2 S}{\partial \eta^2} + d\left(\frac{\partial f}{\partial \eta}\frac{\partial^3 f}{\partial \eta^3}\right) + d\left(\frac{\partial^2 f}{\partial \eta^2}\right)^2 + m_1 f\frac{\partial S}{\partial \eta}, \tag{37}$$

and the Homotopy for this equation is constructed as below

$$(1-p)L_s\left[S(\eta,p) - S_0(\eta)\right] = hp\left\{e\frac{\partial^2 S}{\partial \eta^2} + d\left(\frac{\partial F}{\partial \eta}\frac{\partial^3 F}{\partial \eta^3}\right) + d\left(\frac{\partial^2 F}{\partial \eta^2}\right)^2 + m_1 F\frac{\partial S}{\partial \eta}\right\}, \tag{38}$$

where

$$L_s = \frac{\partial^2}{\partial \eta^2} + \frac{\partial}{\partial \eta}, \tag{39}$$

with boundary conditions

$$S(0,p) = \omega = S_w, S(\infty,p) = 1. \tag{40}$$

Initial approximate solution, $S_0(\eta)$ is chosen in accordance with boundary conditions (40) and satisfying $L_s(S_0) = 0$. Thus we get

$$S_0(\eta) = 1 + (\omega - 1)e^{-\eta}. \tag{41}$$

Repeating as in case of f by using

$$S(\eta,p) = \psi_0(\eta) + \sum_{k=1}^{\infty}\psi_k(\eta). \tag{42}$$

By using $\psi_0(\eta) = S_0(\eta)$, we get all values of ψ's and the graphs are drawn for different values of physical parameter.

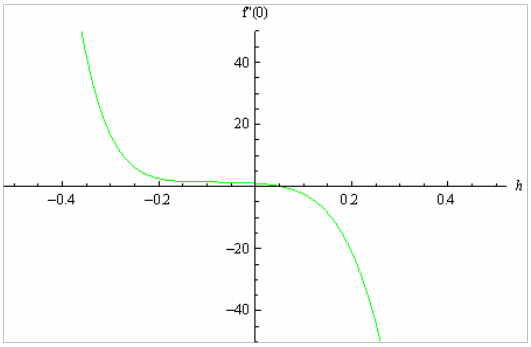

Figure 2: h curve for suction

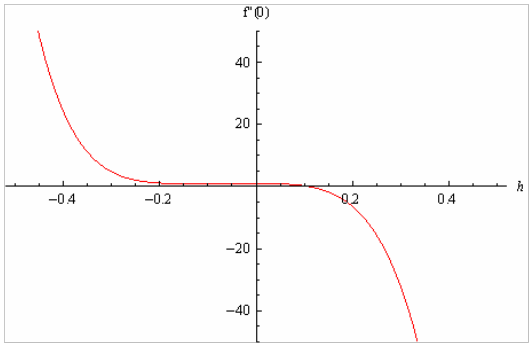

Figure 3: h curve for no suction

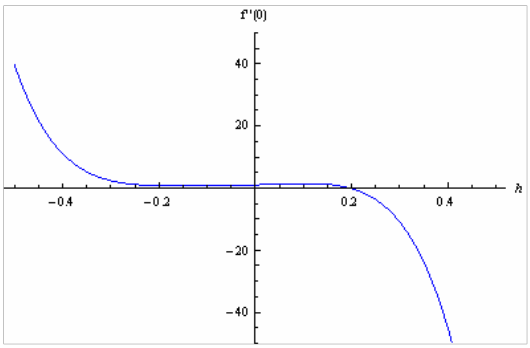

Figure 4: h curve for injection

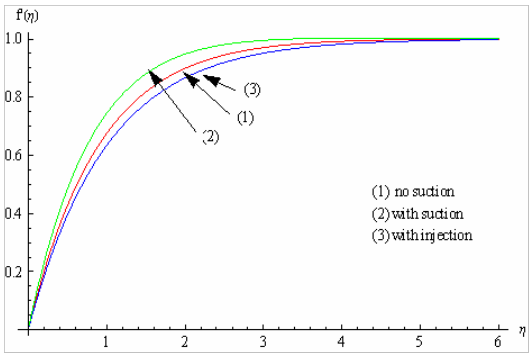

Figure 5: Velocity curves for (1) no suction , (2)suction,(3)injection

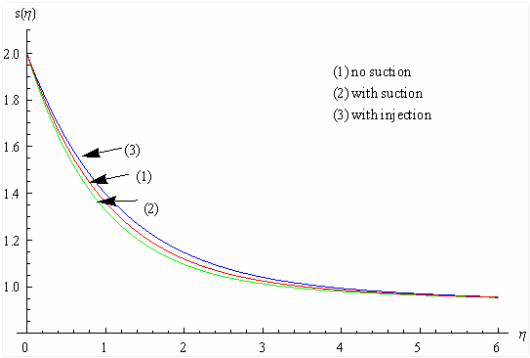

Figure 6: Temperature profiles for (1) no suction,(2)suction, (3)injection

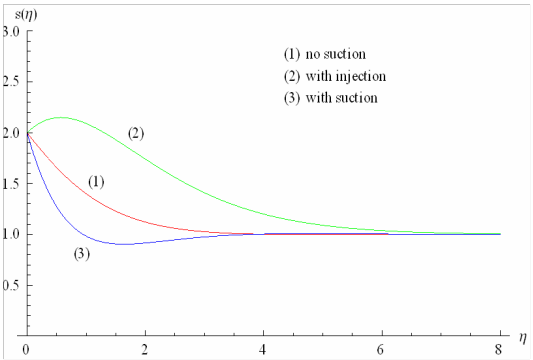

Figure 7: Temperature Profile HAM $\lambda = -2, 0, 2$

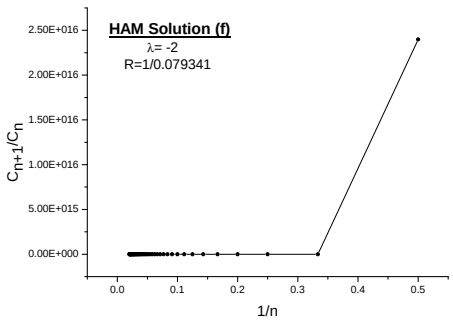

Figure 8: Domb Syke Plot for velocity,

R = 12.60

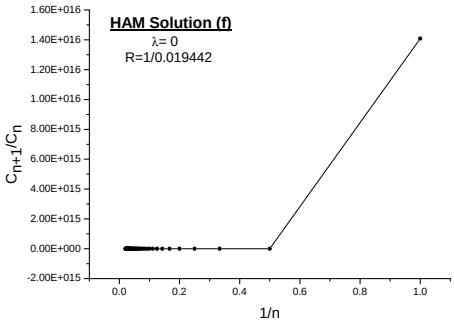

Figure 9: Domb Syke Plot for velocity,

R = 51.44

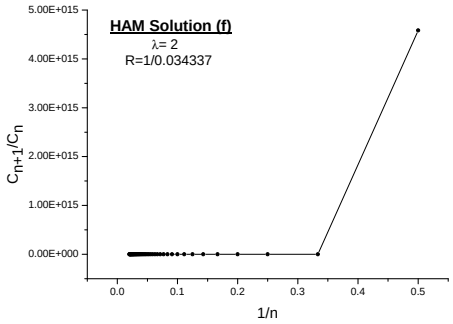

Figure 10: Domb Syke Plot for velocity,

R = 29.12

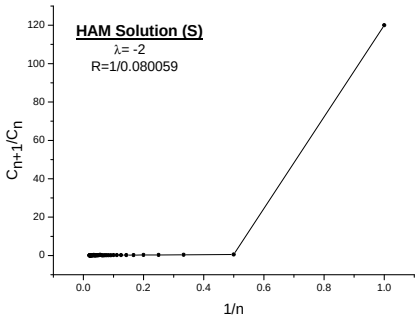

Figure 11: Domb Syke Plot for temperature,

R = 12.49

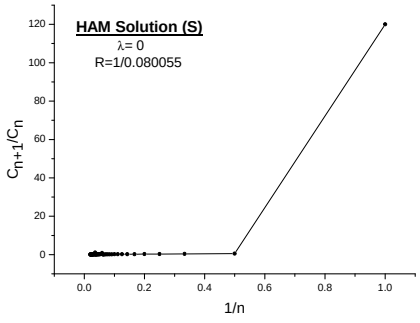

Figure 12: Domb Syke Plot for velocity,

R = 12.49

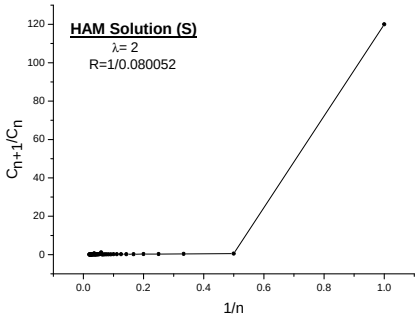

Figure 13: Domb Syke Plot for temperature,

R = 12.49

4 Pade Approximation

When we have only first few terms of an infinite series and the general form of series coefficient say a_n is not transparent, Pade approximants are a good way to approximate the series. Therefore we apply Pade for HAM solution, [4/4] pade for injuction is given by

$$f_{pade} = \frac{-2.2204 \times 10^{-16} - 9.0836 \times 10^{-17}\eta + 0.4999\eta^2 + 0.0355\eta^3 + 0.00713\eta^4}{1.0 + 0.406\eta + 0.06576\eta^2 + 0.0048\eta^3 + 0.0001\eta^4}, \tag{43}$$

[4/4] pade for no suction is given by

$$f_{pade} = \frac{-2.2204 \times 10^{-16} - 9.0836 \times 10^{-17}\eta + 0.4999\eta^2 + 0.0355\eta^3 + 0.0071\eta^4}{1.0 + 0.4061\eta + 0.0657\eta^2 + 0.0048\eta^3 + 0.0001\eta^4}, \tag{44}$$

[4/4] pade for suction is given by

$$f_{pade} = \frac{-2. - 0.8201\eta + 0.3708\eta^2 + 0.0262\eta^3 + 0.0071\eta^4}{1.0 + 0.4100\eta + 0.0670\eta^2 + 0.0049\eta^3 + 0.00012\eta^4}, \tag{45}$$

Pade approximants are able to overcome the finite radius of convergence of the series. The Pade approximants are better than the original series is a common feature. It is based on the assumption that the original function was smoothly varying.

5 Alternate Homotopy Analysis Method (AHAM)

We set $h = -1$ in the zeroth-order deformation equation (12) and introducing a parameter β in the Linear operator $L = \frac{\partial^3}{\partial\eta^3} + \beta\frac{\partial^2}{\partial\eta^2}$ to obtain a alternate Homotopy as

$$(1-p)[f''' + \beta f''] + p\left\{bf''' + m_1 f f'' + m_2\left(c - (f')^2\right)\right\} = 0, \tag{46}$$

subject to the boundary conditions:

$$f(0) = \lambda, f'(0) = 0, f'(\infty) = 1, \tag{47}$$

It is easy to notice that as p deforms from 0 to 1, equation (46) changes from the initial linear equation $f'''(\eta) + \beta\, f''(\eta) = 0$ to the nonlinear equation

$bf''' + m_1 ff'' + m_2\left(c - (f')^2\right) = 0$. Then putting

$$f(\eta) = f_0(\eta) + \sum_{k=1}^{+\infty} f_k(\eta) p^k \tag{48}$$

in (46) and equating the same powers of p , we have:

Zero order:

$$f_o'''(\eta) + \beta f_0''(\eta) = 0, \tag{49}$$

$$f_0(0) = \lambda, f_0'(0) = 0, f_0'(\infty) = 1, \tag{50}$$

First order :

$$f_1''' + \beta f_1'' - f_0''' - \beta f_0'' + b\, f_0''' + m_1 f_0 f_0'' + m_2 c - m_2 f_0' f_0' = 0, \tag{51}$$

Second order :

$$f_2''' + \beta f_2'' - f_1''' - \beta f_1'' + b\, f_1''' + m_1\left(f_0 f_1'' + f_1 f_0''\right) - m_2\left(f_0' f_1' + f_1' f_0'\right) = 0, \tag{52}$$

Third order:

$$f_3'''+\beta f_3''-f_2'''-\beta f_2''+b\, f_2'''+m_1\left(f_0 f_2'' + f_1 f_1'' + f_2 f_0''\right)-m_2\left(f_0' f_2' + f_1' f_1' + f_2' f_0'\right) = 0, \tag{53}$$

Fourth order :

$$\begin{array}{c} f_4'''' + \beta f_4'' - f_3'''' - \beta f_3'' + b\, f_3'''' + m_1\left(f_0 f_3'' + f_1 f_2'' + f_2 f_1'' + f_3 f_0''\right) \\ -m_2\left(f_0' f_3' + f_1' f_2' + f_2' f_1' + f_3' f_0'\right) = 0 \end{array}, \tag{54}$$

and so on, with general boundary condition

$$f_n(0) = 0, f_n'(0) = 0, f_n'(\infty) = 0, n = 1, 2, 3, 4, 5, \ldots\ldots$$

we find the proper values of β in order to make our series solution convergent. Let us consider a physical parameter $f''(0)$, of the problem, which corresponds to wall skin friction.

$$f''(0) = \sum_{0}^{\infty} f_n''(0), \tag{55}$$

If the solution of original nonlinear equation is unique and if the series solution given in equation (48) converges, it should always converge to the same value. Both the series solutions for $f(\eta)$ and $f''(0)$ contain β . Therefore,

we have a family of solutions in terms of β among which we may find the most convergent one using the best value of β . In fact, plotting $f''(0)$ versus β, there should exist a horizontal segment in this plot as long as the solution series given in equation (48) is convergent. Hence, we may find the proper values of β which correspond to this horizontal segment to ensure that our solution is convergent. Using the estimated value of β (fig 14 and fig 15) Graphs of velocity is drawn in fig 16 and it is observed that the curves show same behaviour as in HAM.

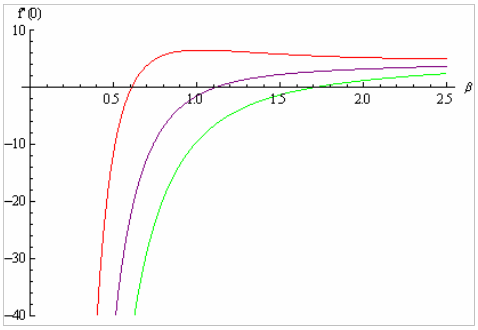

Figure 14: Beta Curves(second order)for velocity for $\lambda < 0, \lambda = 0, \lambda > 0$

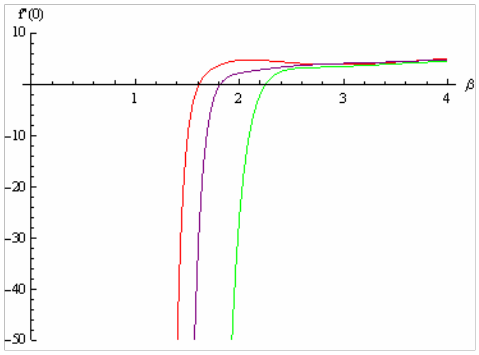

Figure 15: Beta Curves (sixth order) for velocity for $\lambda < 0, \lambda = 0, \lambda > 0$

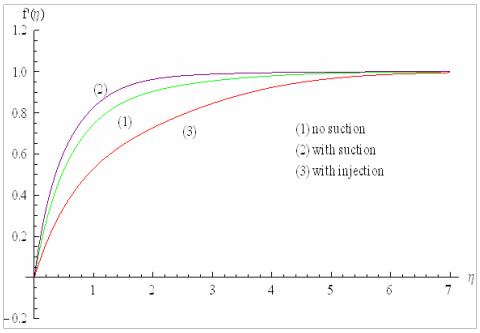

Figure 16: Velocity Profile for AHAM $\lambda < 0, \lambda = 0, \lambda > 0$

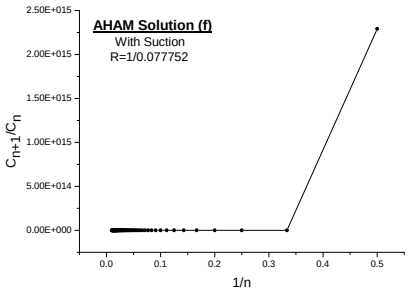

Figure 17: Domb Syke Plot for AHAM velocity, R = 12.90

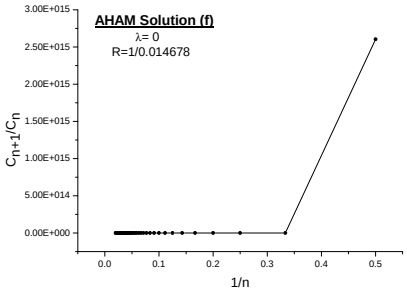

Figure 18: Domb Syke Plot for AHAM velocity, R = 68.13

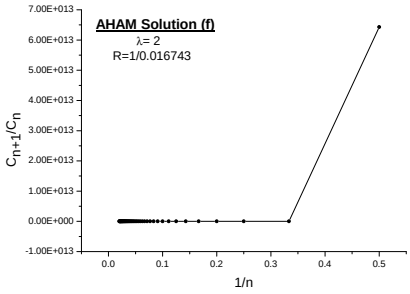

Figure 19: Domb Syke Plot for AHAM velocity, R = 59.73

6 Runge Kutta Merson method

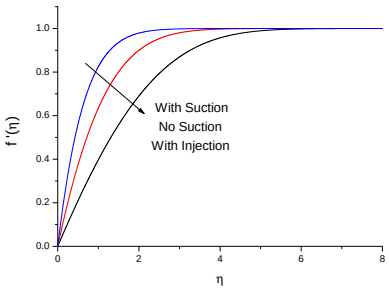

Figure 20: Velocity Profile by RKM

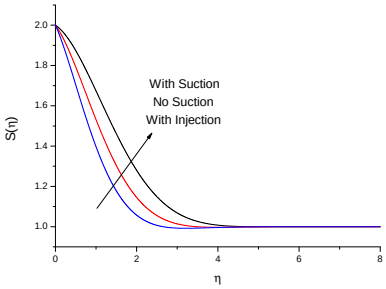

Figure 21: Velocity Profile by RKM $\lambda = -1, \lambda = 0, \lambda = 1$

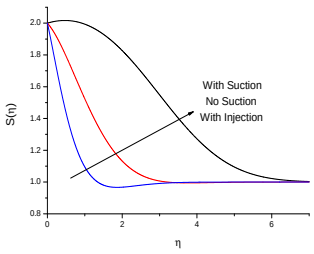

Figure 22: Velocity Profile by RKM $\lambda = -2, \lambda = 0, \lambda = 2$

7 Results and Discussions

In this paper, we have studied two dimensional laminar compressible boundary layer flow with an adverse pressure gradient in the presence of heat and mass transfer. The governing equations are nonlinear PDE and are converted into nonlinear ODE by Falkner Skan transformations. These equations are solved by HAM and AHAM and also numerically by R-K Merson method for the case of heating of wall which corresponds to $S_w = 2$. For HAM solution h-curves are drawn in Figures 2, 3, 4. The range of values are determined and we observe that for h = -0.065 the velocity and temperature curves are giving good congruent solutions. In Figure 5, velocity curves are drawn with suction, no suction, with injection for HAM solution which is comparable with graph of numerical solution obtained by R.K. Merson method and is shown in Figure 20. The velocity expression obtained by HAM is matching with R.K. Merson method. We have also obtained convergence region and radius of convergence by Domb-Sykes Plot (Figure 8 - 10) and it is shown that radius of convergence is R=12.60, 51.44 and 29.12 for $\lambda = -2, 0, 2$ simultaneously. Similarly radius of convergence for suction, no suction and injection is obtained for temperature profile in Figures 11, 12, 13 with R = 12.49. The value of convergence parameter β in AHAM method is obtained by β curves (Figure 14, 15) and using this estimated value of β , velocity curves are drawn in Figure 16 for suction, no suction and injection. The series solution obtained by AHAM is shown to be convergent with radius of convergence as R=12.90 for $\lambda = -2$, R=68.13 for $\lambda = 0$, R=59.73 for $\lambda = 2$ as seen from Figures 17, 18 and 19. We observe that the region of convergence is large AHAM solution than HAM solution. Thus we can conclude that both HAM and AHAM are almost exact solutions. This is also confirmed by comparing them with numerical solution obtained by Runge-Kutta Merson method, (Figure 20, 21, 22).

References

[1] J.D. Anderson, *Hypersonic and High-Temperature Gas Dynamics*, McGraw-Hill, New York, 1989.

[2] Ardeshir Hani, Peter J. Schmid, and Dan S. Henningson, Transient growth in compressible boundary layer flow, *Phys. Fluids*, **8**(3), (1996),826-837.

[3] D. Arnal, Control of laminar-turbulent transition for skin-friction drag reduction in Control of Flow Instabilities and Unsteady Flows, *CISM Course*, (1995), 18-22.

[4] T. Cebeci and A.M.O. Smith, *Analysis of Turbulent Boundary Layers*, Academic Press, New York, 1974.

[5] Ali J. Chamkha, Effects of particulate discussion on the compressible boundary layer flow of a two phase suspension over a horizontal surface, *Journal of Fluids Engineering*, **120**(1), (1998), 146-151.

[6] Yat-Yung Chan, Integral Method in Compressible Laminar Boundary Layers and its Application, *Phys. Fluids*, **9**(1), (1966), 1958-1988.

[7] N. Curle, *The Laminar Boundary Layer Equations*, Clarendon Press, Oxford, 1962.

[8] L. Howarth, On the Solution of the Laminar Boundary Layer, *Proceedings of the Royal Society of London. Series A, Mathematical and Physical Sciences.A*, **164**, (1938), 547-579.

[9] N. Kafoussias and A. Karabis and M. Xenos, Numerical study of two dimensional laminar boundary layer compressible flow with pressure gradient and heat and mass transfer, *International Journal of Engineering Science*, **37,** (1999), 1795 -1812.

[10] G. Kuerti, The laminar boundary layer in compressible Flow, *Advances in Applied Mechanics*, **2**, (1951), 21-92.

[11] M.A. Hossain, L. Pop, Cluj, and T-Y. Na, Michigan, Effect of heat transfer on compressible boundary layer ow over a circular cylinder, *Acta Mechanica*, **131**, (1998), 267-272.

[12] M. Muthanna and G Nath, Laminar compressible boundary layer ow at a three-dimensional stagnation point with vectored mass transfer, *Mathematical Sciences-2, Proc. Indian Acad Sci.*, **5**, (1978), 113-123.

[13] A. Sau and G. Nath, Unsteady compressible boundary layer flow stagnation line of an infinite swept cylinder, *Acta Mechanica*, **108**, (1995), 143-156.

[14] H. Schlichting and J. Kestin, *Boundary-Layer Theory*, Trans., McGraw-Hill New York, 1979.

[15] S. Schreier, *Compressible Flow*, Wiley, New York, 1982.

[16] K. Stewartson, *The Theory of Laminar Boundary Layers in Compressible Fluids*, Oxford, 1964.

[17] B.J. Venkatachala and G. Nath, Compressible Laminar Boundary Layers for Stagnation-Point Flow with Continuous Moving Surfaces, *Acta Mechanica*, **25**, (1976), 145-150.

[18] A.D. Young, Section on boundary layers, in: L. Howarth (Ed.),*Modern Developments in Fluid Mechanics High Speed Flow*, Clarendon Press, Oxford, (1953), 375-475.